

# The miR-17-92 microRNA cluster: a novel diagnostic tool in large B-cell malignancies

Ambrogio Fassina<sup>1</sup>, Filippo Marino<sup>1</sup>, Maayan Siri<sup>1</sup>, Renato Zambello<sup>2</sup>, Laura Ventura<sup>3</sup>, Matteo Fassan<sup>1</sup>, Francesca Simonato<sup>1</sup> and Rocco Cappellesso<sup>1</sup>

Diffuse large B-cell lymphoma (DLBCL) can present as *de novo* or can arise through the transformation of many indolent lymphomas, including follicular lymphoma (FL). The morphological differentiation between germinal center-DLBCL (GC-DLBCL) and high-grade (grade 3) FL could be challenging; the accurate sub-classification of large B-cell lymphomas is mandatory in order to select the most appropriate among the new-targeted therapies. Recent expression profiling studies reported microRNAs (miRNAs) (and miR-17-92 cluster, in particular) as useful tools in differentiating DLBCL and FL. However, these preliminary results are based on cell line-derived data or did not consider grade 3 FL cases. To investigate this point, 36 cases of GC-DLBCL and 18 cases of grade 3 non-transforming FL were considered. All diagnoses were based on the World Health Organization criteria and were confirmed by clinical, histological, and immunohistochemical data. Six members of the miR-17-92 cluster (ie, miR-18b, miR-19b, miR-20a, miR-92, miR-93, and miR-106a) and two control miRNAs (ie, miR-150 and miR-210) were quantified by quantitative reverse transcription-polymerase chain reaction. All the considered miR-17-92 cluster miRNAs were significantly overexpressed in GC-DLBCL, being miR-20a and miR-106a the most dysregulated ( $P < 0.001$ ). Receiver operating characteristics (ROCs) analysis was used to find the optimal cut-off in distinguishing the two histotypes. The ROC estimated thresholds for miR-18b, miR-19b, miR-20a, miR-92, and miR-106a displayed a sensitivity level higher than 0.80 in achieving the GC-DLBCL diagnosis. The classification tree built on the six thresholds allowed the correct identification of 35/36 GC-DLBCL (97.2%). Profiling the miR-17-92 cluster is a promising investigative method for differentiating GC-DLBCL from high-grade FL. Subject to the validation of these findings in further larger studies; miR-17-92 cluster could represent a reliable, standardizable diagnostic tool for the sub-classification of large B-cell lymphoid neoplasm.

Laboratory Investigation (2012) 92, 1574–1582; doi:10.1038/labinvest.2012.129; published online 10 September 2012

**KEYWORDS:** follicular lymphoma; germinal center-diffuse large B-cell lymphoma; miRNA

Diffuse large B-cell lymphoma (DLBCL) is the most common subtype of non-Hodgkin lymphoma in adults worldwide, accounting for approximately 40% of all lymphoid tumors.<sup>1</sup> DLBCL arises from a mature B-cell (usually centroblast or immunoblast) and can present as *de novo* or can arise through the transformation of many indolent lymphomas, including follicular lymphoma (FL).<sup>2,3</sup>

Owing to its pathological heterogeneity, reflected also on the molecular level, and supported by its remarkable variability in clinical presentation, response to treatment, and outcome, DLBCL is considered a group of diseases rather than a single entity.<sup>4</sup> Gene expression and immunohistochemical (IHC)

studies have successfully sub-classified DLBCL in two major groups, namely the germinal center-DLBCL (GC-DLBCL) and the activated B-cell-like-DLBCL (ABC-DLBCL).<sup>5,6</sup> The GC-DLBCL phenotype is characterized by a more indolent course than ABC-DLBCL.<sup>7</sup> On morphological and IHC level, the differentiation between GC-DLBCL and non-transforming high-grade (grade 3) FL (considered as a GC tumor) is challenging, and new diagnostic tools are warranted in the clinicopathological management of these patients, because of prognostic and therapeutic implications.<sup>7–14</sup>

MicroRNAs (miRNAs) are a class of short non-coding single-stranded RNAs, which regulate gene expression by

<sup>1</sup>Department of Medicine, Surgical Pathology and Cytopathology Unit, University of Padua, Padua, Italy; <sup>2</sup>Department of Medicine, Hematology Unit, University Hospital of Padua, Padua, Italy and <sup>3</sup>Department of Statistical Sciences, University of Padua, Padua, Italy  
Correspondence: Dr M Fassan, MD, Department of Medicine, Surgical Pathology and Cytopathology Unit, University of Padua, Via Aristide Gabelli, 61; 35121, Padua, Italy.

E-mail: matteo.fassan@gmail.com

Received 8 May 2012; revised 2 July 2012; accepted 23 July 2012

targeting messenger RNAs and triggering either the repression of their translation or their degradation.<sup>15</sup> MiRNAs are involved in several biological pathways, including development, cell proliferation, differentiation, and apoptosis and have been considered as a promising new class of biomarkers for tumor diagnosis and prognosis.<sup>16</sup>

Recently, several reports have investigated miRNAs expression profiling in differentiating GC-B-cell lymphomas (BCLs), focusing on DLBCL and high-grade FL in particular.<sup>17–19</sup> Copy number abnormalities, MYC activity, and the genetic fingerprint of normal B cells mechanistically define the miRNA profile of DLBCL.<sup>20</sup> Among others, several miRNAs of the miR-17-92 cluster have been demonstrated to be the most promising.<sup>17–20</sup> The miR-17-92 cluster, located at chromosome locus 13q31.3, consists of six miRNAs (miR-17, miR-18a, miR-19a, miR-20a, miR-19b, and miR-92a) and two paralogs (the miR-106b-25 cluster on chromosome 7 and the miR-106a-363 cluster on chromosome X).<sup>21,22</sup> A large volume of experimental data demonstrated the oncogenic role of miR-17-92 cluster in both hematopoietic malignancies and solid tumors, being involved in the regulation of cell cycle and cell death.<sup>23–26</sup>

Despite the important role demonstrated for the miR-17-92 cluster, no study has previously assessed its diagnostic value in differentiating GC-DLBCL from high-grade (G3; non-transforming) FL. In the present work, we investigated a cohort of patients with large BCL, comparing the differences in miRNA expression.

## MATERIALS AND METHODS

### Patients and Tissue Specimens

Tissue samples of 36 cases of *de novo* GC-DLBCL (ie, with no clinical history of indolent lymphoma, or coexisting FL areas at diagnosis) and 18 of high-grade (grade 3) non-transforming FL reported between 2005 and 2009 were retrieved from the archives of the Surgical Pathology and Cytopathology Unit of the University of Padua and included in the study (Table 1). In particular, to prevent intra-specimen variability, FL cases were selected considering only cases with diffuse areas proportion <25% (ie, FL follicular pattern; Figures 1a and b) and which were diffusely grade 3 (ie, grade 3: >75% of the neoplastic area).<sup>27,28</sup> All diagnoses were based on the World Health Organization criteria and

confirmed in all instances by two pathologists (FM and AF) by clinical, histological, and IHC data.<sup>27,28</sup> Five lymph nodes with minor reactive changes, obtained by sleeve gastrectomies for the treatment of obesity, were included as non-neoplastic lymphatic tissue (N). The University Hospital of Padua institute's ethical regulations on research conducted on human tissues were followed.

### Ethic Statement

Written informed consent was obtained from all participants involved in the study and the study was approved by the institutional review board of the University Hospital of Padua (Azienda Ospedaliera di Padova—Università degli Studi di Padova).

### Immunohistochemistry

Immunohistochemistry was performed on 4–5  $\mu\text{m}$ -thick formalin-fixed and paraffin-embedded (FFPE) sections from each tumor sample. Using the standard avidin-biotin-peroxidase complex method, staining was done automatically (Bondmax, Menarini, Florence, Italy), as described elsewhere,<sup>29,30</sup> for an accepted panel of IHC markers, according to the manufacturer's instructions: (i) BCL2 (clone 124; Dako, Glostrup, Denmark; working dilution 1:200, 30 min, citrate buffer); (ii) CD10 (clone 56C6; Diagnostic BioSystems, Pleasanton, CA, USA; working dilution 1:50, 30 min, citrate buffer); (iii) CD5 (clone 4C7; Dako; working dilution 1:50, 30 min, citrate buffer); (iv) CD21 (clone 1F8; Dako; working dilution 1:100, 30 min, citrate buffer); (v) CD23 (clone 1B12; Hot Springs, AR, USA; working dilution 1:25, 60 min, citrate buffer); (vi) BCL-6 (clone PG-B6p; Dako; working dilution 1:100 30 min, EDTA); (vii) MUM1 (clone MUM1p; Dako; working dilution 1:50, 20 min, citrate buffer); and (viii) cyclin D1 (clone EP12; Dako; working dilution 1:20, 20 min, citrate buffer).<sup>7</sup> Sections were then slightly counterstained with hematoxylin. Appropriate positive and negative controls were run concurrently. The expression of each IHC marker was jointly scored by three of the authors (FM, AF, and RC) and dichotomized as positive or negative.

### B-Cell Clonality

B-cell clonality was evaluated by the detection of Ig genes rearrangement, using the B-cell lymphoma kit<sup>TM</sup> (Experteam,

**Table 1 Clinical and immunohistochemical characteristics of the considered series**

Histotype	Sex (M/F)	Age Mean $\pm$ s.d.	Ann Arbor stage				Immunohistochemistry					
			I	II	III	IV	CD5	CD10	Bcl2	Bcl6	MUM1	Cyclin D1
FL	12/6	65.9 $\pm$ 13.7	3 (16.7%)	3 (16.7%)	6 (33.3%)	6 (33.3%)	0 (0.0%)	17 (94.4%)	14 (77.8%)	18 (100.0%)	0 (0.0%)	0 (0.0%)
DLBCL	13/23	65.8 $\pm$ 16.5	5 (13.9%)	6 (16.7%)	9 (25.0%)	16 (44.4%)	0 (0.0%)	36 (100.0%)	15 (41.7%)	36 (100.0%)	0 (0.0%)	0 (0.0%)

Abbreviations: DLBCL, diffuse large B-cell lymphoma; F, female; FL, follicular lymphoma; M, male.

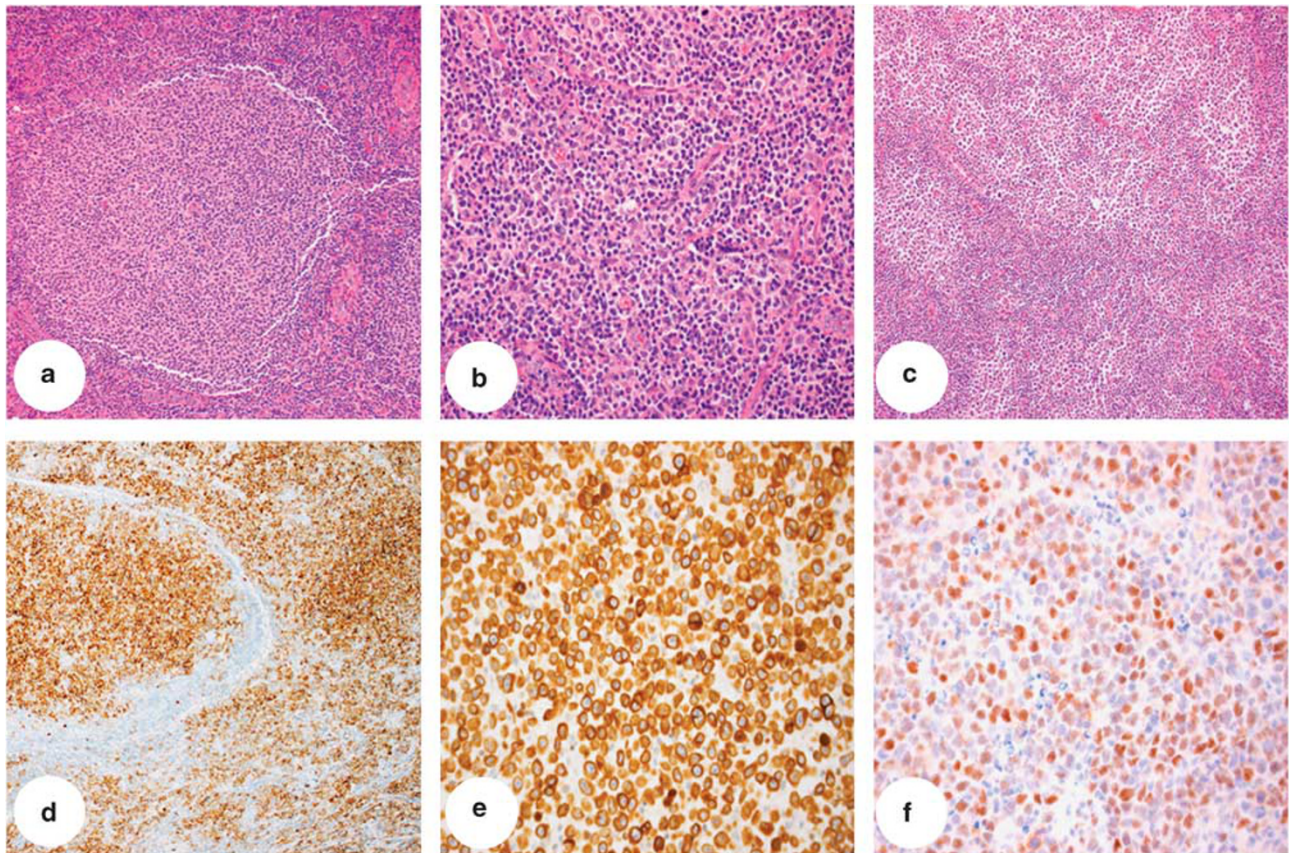


**Figure 1** Representative histological and immunohistochemical images obtained from the considered series. (a, b) Non-transforming follicular lymphoma (grade 3; hematoxylin and eosin (H&E) stain) showing the typical proliferation of small centrocytes arranged in a follicle. (c) Germinal center-diffuse large B-cell lymphoma (GC-DLBCL) with complete effacement of nodal architecture because of diffuse infiltrates of large blast lymphoid cells (GC-DLBCL; H&E stain). Representative immunostain for CD10 (d), B-cell lymphoma (BCL)-2 (e), and BCL-6 (f) in GC-DLBCL cases. (Original magnifications  $\times 20$  and  $\times 40$ ).

Venice, Italy). In all cases, 5  $\mu\text{m}$  thick sections were obtained from FFPE tissues of each neoplastic/non-neoplastic sample. Genomic DNA was extracted from these sections previously digested with proteinase K. Ig chain gene clonality was evaluated according to the manufacturer's instructions.

### MiRNA Selection

Recent expression profiling studies identified members of the miR-17-92 cluster (ie, miR-19b, miR-20a, and miR-92) and three of its paralogs (ie, miR18b, miR-93, and miR-106a) as useful biomarkers in differentiating DLBCL from low-grade FL.<sup>17-19</sup> Consequently, the diagnostic performance of these miRNAs was explored in our series of GC-DLBCL and high-grade (grade 3) non-transforming FL. To further support the qRT-PCR data, both miR-150 and miR-210 were selected as controls: (i) miR-150 has been reported to be a key regulator of normal hematopoiesis targeting *MYB*, being downregulated in lymphoid neoplasm;<sup>31</sup> (ii) miR-210 has been demonstrated to be an oncomiR involved in the cell cycle and considered to be overexpressed in many tumors, as well as lymphomas.<sup>32</sup>

### RNA Extraction

Using a sterile Harris Micro-Punch™ (Sigma-Aldrich, St Louis, MO, USA), 2-mm tissue cores were obtained from the paraffin block of each tumor/normal sample. Total RNA was extracted using the RecoverAll kit (Ambion, Austin, TX, USA), as reported elsewhere.<sup>33</sup> The sample was then grinded on dry ice, placed in a 1.5 ml microcentrifuge tube containing 1 ml of xylene, vortexed and incubated at 50 °C for 3 min to melt the paraffin. The material was then centrifuged at 14 000 r.p.m. for 10 min at room temperature to pellet the specimen, after which the xylene was carefully removed and the pellet was washed three times with 1 ml of 100% room temperature ethanol. The pellet was then air-dried at room temperature for 45 min. Following deparaffinization, tissue was protease digested by incubating the pellet in 200  $\mu\text{l}$  digestion buffer and 4  $\mu\text{l}$  protease at 80 °C for 15 min. For total RNA isolation, 240  $\mu\text{l}$  of isolation additive was added to the sample, followed by vortexing and addition of 550  $\mu\text{l}$  of 100% ethanol. The mixture was then loaded onto a prepared filter and collection tube according to the manufacturer-supplied procedure. The sample was centrifuged for 30 s at 10 000 r.p.m. Flow through was discarded and filter washed

twice with wash buffer. Nuclease digestion was obtained by adding 60  $\mu$ l DNase master mix (containing 6  $\mu$ l 10  $\times$  DNase buffer, 4  $\mu$ l DNase, 50  $\mu$ l nuclease-free water) to the center of the filter and incubated for 30 min at room temperature. The filter was subsequently washed three times according to the manufacturer's protocol, and RNA was eluted with 60  $\mu$ l preheated nuclease-free water. RNA quality and quantity was measured by Nanodrop technology (Thermo Scientific, Wilmington, DE, USA). The eluted RNAs were immediately aliquoted (into 20  $\mu$ l volumes) and stored at  $-80^{\circ}\text{C}$  until all extractions were completed. To avoid any potential variation between assays, analyses were carried out on all of the extracts simultaneously.

### Reverse Transcription and Quantitative Real-Time PCR

To detect and quantify mature miRNAs, the NCode<sup>TM</sup> miRNA quantitative real-time PCR (qRT-PCR) method (Invitrogen, Carlsbad, CA, USA) was applied according to the manufacturer's instructions. Reverse transcription (RT) and poly(A) tailing reactions were performed with 4  $\mu$ l 5  $\times$  reaction mix, 2  $\mu$ l 10  $\times$  SuperScript enzyme mix, and 500 ng of total RNA in a final volume of 20  $\mu$ l. The mixture was incubated at 37  $^{\circ}\text{C}$  for 60 min. Following RT steps, qRT-PCR was performed: 2  $\mu$ l of the RT product was transferred into a PCR reaction mixture consisting of 10  $\mu$ l Express SYBR green qPCR SuperMix with premixed ROX, 0.4  $\mu$ l miRNA-specific forward primer (10  $\mu\text{M}$ ; primers sequence in Table 2), 0.4  $\mu$ l universal qPCR primer (10  $\mu\text{M}$ ) in a final volume of 20  $\mu$ l. qRT-PCR cycling began with template denaturation and hot start Taq activation at 95  $^{\circ}\text{C}$  for 2 min, then 45 cycles of 95  $^{\circ}\text{C}$  for 15 s, and 60  $^{\circ}\text{C}$  for 1 min performed in a LightCycler 480 Real-Time System (Roche Diagnostics, Mannheim, Germany). Normalization was done with the small nuclear RNA U6B (RNU6B, Invitrogen). All the reactions were run in triplicate, including no-template controls. Normalized expression was calculated using the comparative Ct method

**Table 2 Primers used for the quantitative reverse transcription-polymerase chain reaction analysis**

Gene of interest	Forward primer (5'–3')
<i>hsa-miR-150</i>	CTCCCAACCCCTGTACCAAGT
<i>hsa-miR-210</i>	CGTGTGACAGCGGCTGA
<i>miR-17-92 microRNA cluster and paralogs</i>	
<i>hsa-miR-18b</i>	GCTAAGGTGCATCTAGTGCAGTTAG
<i>hsa-miR-19b</i>	GCAAATCCATGCAAACTGA
<i>hsa-miR-20a</i>	CGGTAAAGTGCTTATAGTGCAGGTAG
<i>hsa-miR-92a</i>	CACCTGTCCCGGCTGT
<i>hsa-miR-93</i>	AAGTGCTGTTCGTGCAGGTAG
<i>hsa-miR-106a</i>	GAAAAGTGCTTACAGTGCAGGTAG
<i>Housekeeping gene</i>	
<i>RNU6B</i>	ACGCAAATTCGTGAAGCGTT

and fold change was derived from the equation  $2^{-\Delta\Delta\text{Ct}}$  for each miRNA.

### Statistical Analysis

Differential expression was tested for all single miRNA species using two-sided *t*-test, after checking both the assumption of normality (Shapiro–Wilk's test) and the assumption of homogeneity of variance (F-test). Receiver operating characteristics (ROCs) analysis was used to find out the optimal cut-offs for miRNAs' expression for stratifying cases according to their final histopathological diagnosis (GC-DLBCL vs high-grade FL). A classification tree was trained on a prefiltered set of miRNA profiles. MiRNAs were considered only if they were significantly differentiated among GC-DLBCL and high-grade FL. The classification tree was calculated using the Euclidean distance. A *P*-value  $< 0.05$  was considered statistically significant. All statistical analyses were performed using the R software (R Development Core Team, version 2.9; R Foundation for Statistical Computing, Vienna, Austria; www.R-project.org).

## RESULTS

### Clinical-Pathological Characteristics of the Patients' Series

Overall, the male/female ratio was 13/23 for GC-DLBCL and 12/6 for high-grade FL; patients mean age was  $65.8 \pm 16.5$  years (median 71; range 21–77) for GC-DLBCL and  $65.9 \pm 13.7$  years (median 68; range 40–90) for high-grade FL. Cases were distributed according Ann Arbor stages as follows: 3 stage I (16.7%), 3 stage II (16.7%), 6 stage III (33.3%), 6 stage IV (33.3%), for FL; 5 stage I (13.9%), 6 stage II (16.7%), 9 stage III (25.0%), 16 stage IV (44.4%), for DLBCL Table 1. Ig chain genes were clonally rearranged in all lymphomas and in none of the *N* cases. In high-grade FL, 11 cases were classified as grade 3a FL ( $> 15$  centroblast/hpf with centrocytes) and 7 cases as grade 3b FL ( $> 15$  centroblast/hpf without centrocytes). GC-DLBCL cases displayed complete or partial nodal architecture effacement by diffuse infiltrates of large blast lymphoid cells (Figure 1c). Among high-grade FL, 17 cases (94.4%) consistently expressed CD10; all cases were positive for BCL-6 in at least a proportion of tumor cells, and negative for CD5, MUM1, and cyclin D1; 14 cases (77.8%) expressed BCL-2 protein. In agreement with *Hans algorithm*, all GC-DLBCL displayed strong and diffuse immunostain for CD10 and BCL-6 protein (Figures 1d and f) and lack of immunostain for MUM1.<sup>7</sup> BCL-2 protein was expressed in 15 GC-DLBCL (41.7%; Figure 1e), and all the tumors lacked an expression of either CD5 or Cyclin D1. In FL, follicular dendritic cells (FDC) are important to the microenvironment in which FL cells grow, as a result we performed IHC analysis with monoclonal antibodies for CD21 and CD23, markers of FDC.<sup>34</sup> Both antibodies (CD21 mostly negative in the neoplastic counterpart, whereas CD23 was variably positive also in FL neoplastic cells) irregularly highlighted, in FL cases, the remnants of the FDC network,

which was always absent or arranged at the periphery of the neoplastic areas in DLBCL cases. Moreover, the lack of any CD21 and CD23 immunoreaction in DLBCL cases highlighted the absence of evident follicular areas, supporting the final diagnosis of *de novo* DLBCL.

### MiRNA Expression is Dysregulated Among GC-DLBCL, High-Grade FL, and Non-Neoplastic Lymphoid Tissue

The six miR-17-92 cluster miRNAs, even with limited differences in fold changes, were significantly overexpressed in GC-DLBCL compared with grade 3 FL (all  $P < 0.05$ ; Figure 2; Table 3), being miR-20a and miR-106a the most

dysregulated ( $P < 0.001$ ; Figure 2; Table 3). The expression levels of miR-150 and miR-210 were similar in the GC-DLBCL and grade 3 FL groups (Figure 2; Table 3).

Notably, GC-DLBCL also showed significantly higher levels of the six miR-17-92 cluster miRNAs than N (all  $P < 0.05$ ; Figure 2; Table 3). Only miR-18b was significantly overexpressed in high-grade FL in comparison with N ( $P = 0.001$ ; Figure 2; Table 3), whereas the other five miR-17-92 cluster miRNAs showed a trend in overexpression in comparison with N (Table 3).

As expected, in both GC-DLBCL and high-grade FL, miR-210 showed higher expression levels in lymphomas than in N (both  $P < 0.001$ ; Figure 2; Table 3); conversely, miR-150

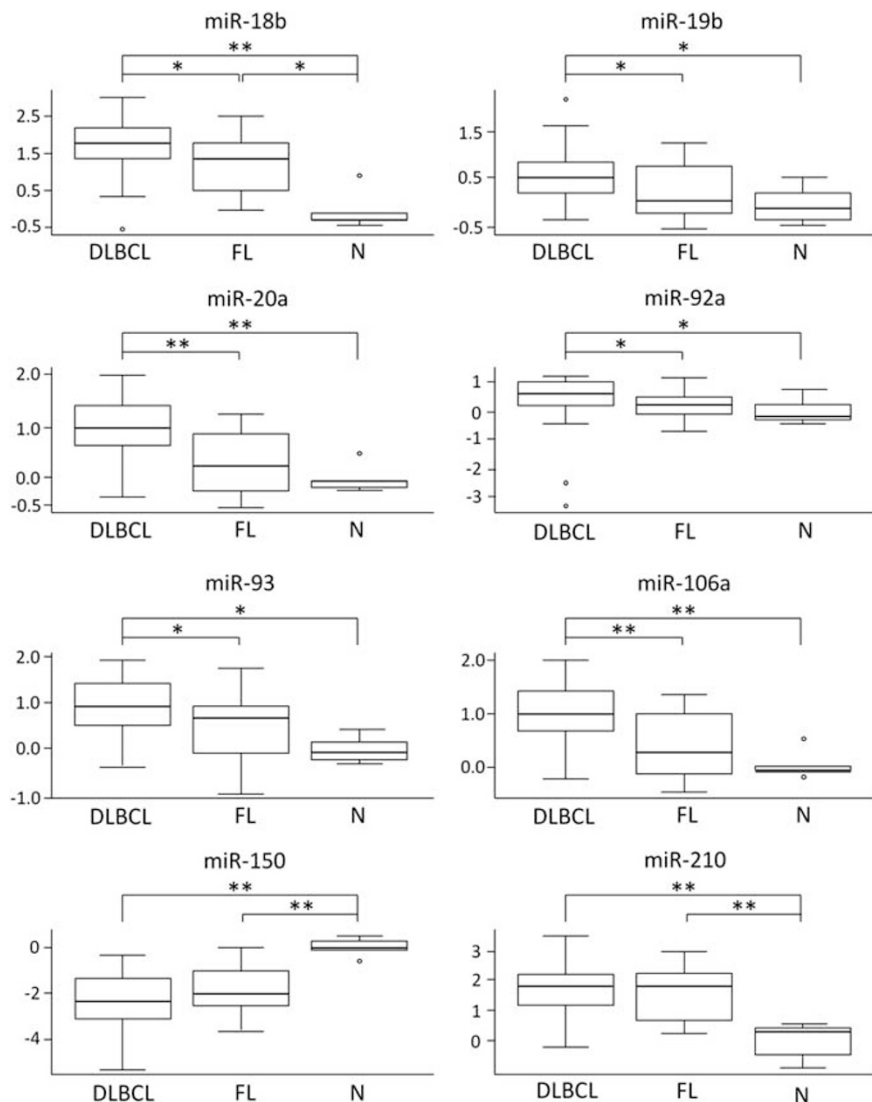


**Figure 2** miR-17-92 microRNAs (miRNAs) cluster is differently expressed among germinal center (GC) large B-cell lymphomas. Box plots show difference in miRNAs expression between GC-diffuse large B-cell lymphomas (DLBCL), non-transforming follicular cell lymphomas (grade 3; FL), and non-tumor lymph-nodes (N). The six miR-17-92 cluster miRNAs were significantly overexpressed between DLBCL and grade 3 FL (all  $P < 0.05$ ), being miR-20a and miR-106a the most dysregulated ( $P < 0.001$ ). The expression levels of miR-150 and miR-210 were similar in these two groups. X axis: the three different histological groups considered in the analysis (DLBCL, FL, and N); Y axis: miRNAs relative expression levels (logarithmic scale). \* $P < 0.05$ ; \*\* $P < 0.001$ .

was downregulated in tumor samples in comparison with *N* (both  $P < 0.001$ ; Figure 2; Table 3).

No significant difference in miRNAs expression was observed among the 11 grade 3a and the 7 grade 3b FL cases and according to other clinicopathological characteristics (ie, Ann Arbor stage, age, and sex).

**Table 3 MicroRNAs expression differences between GC-DLBCLs, high-grade non-transforming FL, and *N***

miRNA	GC-DLBCL vs FL		GC-DLBCL vs <i>N</i>		FL vs <i>N</i>	
	Fold change	<i>P</i> -value <sup>a</sup>	Fold change	<i>P</i> -value <sup>a</sup>	Fold change	<i>P</i> -value <sup>a</sup>
<i>hsa-miR-150</i>	0.7	0.078	0.1	<b>&lt;0.001</b>	0.2	<b>&lt;0.001</b>
<i>hsa-miR-210</i>	1.1	0.737	6.6	<b>&lt;0.001</b>	6.1	<b>&lt;0.001</b>
<i>hsa-miR-18b</i>	1.6	<b>0.022</b>	6.5	<b>&lt;0.001</b>	4.0	<b>0.001</b>
<i>hsa-miR-19b</i>	1.5	<b>0.041</b>	2.1	<b>0.031</b>	1.4	0.410
<i>hsa-miR-20a</i>	2.0	<b>&lt;0.001</b>	3.1	<b>&lt;0.001</b>	1.5	0.270
<i>hsa-miR-92a</i>	1.5	<b>0.039</b>	1.8	<b>0.030</b>	1.2	0.390
<i>hsa-miR-93</i>	1.4	<b>0.026</b>	2.8	<b>0.001</b>	2.0	0.120
<i>hsa-miR-106a</i>	1.9	<b>&lt;0.001</b>	3.1	<b>&lt;0.001</b>	1.6	0.202

Abbreviations: GC-DLBCL, germinal center-diffuse large B-cell lymphoma; FL, follicular lymphoma, *N*, control cases.  
<sup>a</sup>T-test; in bold = statistically significant.

**MiR-17-92 Cluster Differentiate Between GC-DLBCL and High-Grade FL**

ROC curves of miR-17-92 miRNA cluster expression were calculated to determine threshold, sensitivity, and specificity in distinguishing GC-DLBCL from high-grade FL. All these miRNAs were suitable to discriminate between the two groups, with a *P*-value  $< 0.05$  (Table 4).

The thresholds estimated for miR-18b, miR-19b, miR-20a, and miR-106a displayed sensitivity  $> 0.80$  in confirming a GC-DLBCL diagnosis (Figure 3a; Table 4). Conversely, only miR-92a and miR-93 thresholds demonstrated specificity  $> 0.80$  (0.89 and 0.83, respectively; Figure 3a; Table 4).

The classification tree built on miR-17-92 miRNA cluster expression profiles displayed that altogether the obtained

**Table 4 ROC curve of the miR-17-92 miRNAs considered**

miRNA	AUC	<i>P</i> -value	Threshold	Specificity	Sensitivity
<i>hsa-miR-18b</i>	0.70	0.011	1.05	0.44	0.91
<i>hsa-miR-19b</i>	0.66	0.030	0.11	0.55	0.82
<i>hsa-miR-20a</i>	0.79	$<0.001$	0.26	0.61	0.92
<i>hsa-miR-92a</i>	0.75	0.001	0.63	0.89	0.60
<i>hsa-miR-93</i>	0.66	0.030	1.02	0.83	0.47
<i>hsa-miR-106a</i>	0.79	$<0.001$	0.43	0.61	0.89

Abbreviations: AUC, area under the curve; miRNA, microRNA; ROC, receiver operating characteristic.

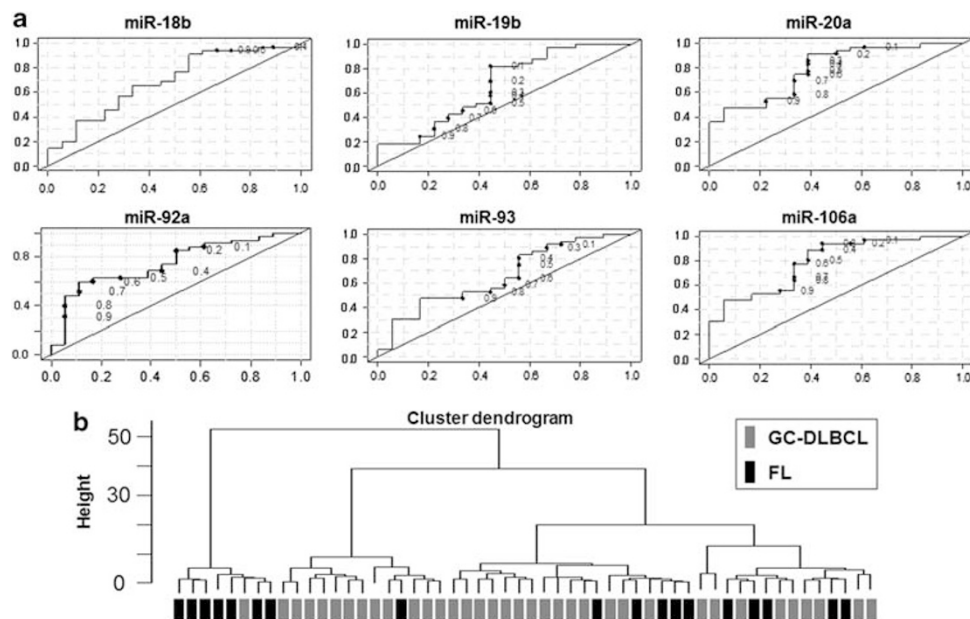


**Figure 3** miRNAs could differentiate among BCLs (germinal center-diffuse large B-cell lymphomas (GC-DLBCLs) and grade 3 non-transforming follicular lymphomas (FLs)). (a) Receiver operating characteristic (ROC) curves of the miR-17-92 miRNAs considered. ROC curves were calculated to determine threshold, sensitivity, and specificity in GC-DLBCL vs high-grade FL. All the considered miRNAs can significantly discriminate between the two groups, with a *P*-value  $< 0.05$ . X axis: false-positive rate; Y axis: true-positive rate. (b) Classification tree trained on the miR17-92 miRNAs profiles displaying that altogether the obtained thresholds allowed to correctly identify 35/36 GC-DLBCL (97.2%).

thresholds allowed to correctly identify 35/36 GC-DLBCL (97.2%; Figure 3b).

## DISCUSSION

DLBCL is a heterogeneous group of lymphomas consisting of large size solid sheets of transformed B cells, mainly resembling normal immunoblasts or centroblasts, with a partial/complete effacement of lymph node architecture.<sup>27,28</sup> Immunoblasts are large cells with single prominent nucleolus and abundant cytoplasm often with plasmocytoid appearance. Centroblasts present as large, non-cleaved cells with round/oval nuclei, multiple nucleoli, vesicular chromatin, and basophilic cytoplasm.<sup>27,28</sup> These last cellular features may overlap those of grade 3 FL, in which the proportion of centrocytes (small/medium sized cells with cleaved nuclei, inconspicuous nucleoli, and scant cytoplasm) and centroblasts varies up to the complete absence of centrocytes.<sup>27,28</sup> Moreover, in the presence of diffuse areas (>25%) of blastic cells in a grade 3 FL, the cases have been proposed to be referred as a full-blown DLBCL.<sup>27,28,35</sup>

Also by the molecular point of view, DLBCL includes genetic and molecular alterations often shared with high-grade FL. Both these lymphomas generally express B-cell antigens (CD-19, CD-20, and CD-79a), surface/cytoplasmic immunoglobulin, and (in various proportions) CD10, BCL-2 protein, and BCL-6 protein.<sup>16,36–38</sup> DLBCL may also share with high-grade FL the t(14;18) translocation, which results with an overexpression of the *BCL-2* oncogene,<sup>39–42</sup> and abnormalities involving the *BCL-6* gene, which encodes an essential transcription factor for the GC development.<sup>43,44</sup> Thus, the morphological/molecular differentiation between DLBCL (GC subtype in particular) and grade 3 FL could be challenging.

By the clinical point of view, grade 3 FL are mostly treated as an aggressive disease, as DLBCL.<sup>8</sup> More recently, some authors are proposing to consider the 3a group as an indolent BCL and the 3b as clinically similar to DLBCL, but conflicting data have been published.<sup>8</sup> In fact, in contrast to DLBCL, the relapse rate of grade 3b FL is in some series higher and survival is longer.<sup>9,10,45</sup> Moreover, several reports have found no difference in outcome between FL grades 3a and 3b when treated with anthracycline-based therapy, and molecular studies identified comparable gene expression profiles between FL grade 3a and FL grade 3b.<sup>11–14</sup> These findings, the advent of new-targeted therapies, and the clinical follow-up with limited sampling of the disease (ie, peripheral blood, fine needle aspiration biopsies) strictly demand new diagnostic tools able to differentiate such similar diseases.

Recent reports have demonstrated the diagnostic impact of miRNAs in human pathology.<sup>15,46</sup> Owing to their structural characteristics, miRNAs are, in contrast to most mRNAs, very stable *in vitro* and long-lived *in vivo*, which might be critical in a clinical setting and allow analysis of samples obtained from different sources (ie, urine, blood, FFPE tissues).<sup>16</sup> Some recent articles investigated the diagnostic feasibility of

miRNAs in discerning among large BCLs, and have established specific miRNA signatures able to differentiate these tumors.<sup>17–19</sup>

Among the others, some authors investigated the different miRNA profiles between DLBCL and FL. However, these preliminary results are based on cell line-derived data or considering grade 1 and 2 FL (and not grade 3), affecting a comprehensive comparison among studies.<sup>17–19</sup> Thus, the aim of this study was to differentiate two morphologically and molecularly similar nosological entities as GC-DLBCL and high-grade (G3) FL, using miRNA expression analysis, in the search of additional diagnostic tools to be used in daily pathology routine.<sup>47</sup>

Seminal works highlighted the components of the miR-17-92 cluster, as some of the most dysregulated miRNAs in both DLBCL and FL.<sup>17–19</sup> Moreover, this cluster owns a recognized oncogenic potential in lymphoid malignancies.<sup>22,48</sup> He *et al*<sup>48</sup> demonstrated that lentiviral transduction of the miR-17-92 cluster into hematopoietic cells dramatically accelerates lymphomagenesis in *MYC* transgenic mice. Of interest, the *MYC* oncogene has been recently shown to upregulate the expression of the miR-17-92 cluster and emerged as a key regulator of the miRNA profile in DLBCL.<sup>20</sup> In humans, chromosomal amplification at 13q31-q32 leads to the cluster's miRNAs overexpression (the *chromosome 13 open reading frame 25* gene; *C13orf25*) in several BCLs, including DLBCL and high-grade FL.<sup>48–50</sup>

The biological importance of the miR-17-92 cluster is further underlined by the presence of its paralogs on chromosomes 7 and X: these miRNAs, located in different chromosomes, derive from a unique gene that underwent a series of dysregulations (duplications, mutations, and loss) during the early evolution of vertebrates.<sup>22</sup> Interestingly, the miRNAs in the cluster do not vary entirely in parallel with each other in B-cell lines, suggesting that either the processing or the stability of these miRNAs are differently regulated, and supporting the fact that only some of the cluster's components have been detected as dysregulated in large BCLs.<sup>51</sup>

Thus, we decided to test miR-17-92 cluster feasibility as a useful diagnostic tool in differentiating DLBCL and high-grade FL. In our series, as expected, we observed a consistent overexpression of all the six miR-17-92 miRNAs tested in DLBCL and FL in comparison with the control lymphoid tissue.<sup>48</sup> The lack of statistical significance for five out of six miRNAs in the FL group should be related to the relatively small number of control tissue samples. However, the six miRNAs signature significantly discriminates the two different histopathological categories, and the classification tree built on the obtained ROC curves allowed a correct identification of the 97% of GC-DLBCL cases. Among the others, miR-20a and miR-106a showed the most significant differences in expression levels between DLBCL and FL cases, supporting the notion that the different miR-17-92 cluster elements are not concurrently dysregulated.<sup>51</sup>

Overexpression of miR-17-92 cluster members in GC-DLBCL in comparison with high-grade FL, further supports the oncogenic potential of these miRNAs. In fact, DLBCL could represent a more de-differentiated form in FL natural history. Lawrie *et al*<sup>17</sup> described among *de novo* and transformed DLBCL cases a FL transformed-specific miRNAs signature, which was characterized by the dysregulation of four of the members of the miR-17-92 cluster. In the Lawrie's study, miR-17-92 miRNAs expression levels were comparable between FL cases that subsequently underwent DLBCL transformation and those that did not, suggesting a late involvement of the miR-17-92 cluster only in the acquisition of a more biologically aggressive phenotype.<sup>17</sup> Further larger prospective studies are needed to confirm these data, and to investigate the possible role of miR-17-92 in FL transformation in GC-DLBCL, focusing not only on miR-17-92 diagnostic value, but also on its prognostic potentials.

The present results further show that miRNA profiling may be helpful in differentiating large BCLs. The identification of histotype-specific miRNA signature offers an exciting new insight into the molecular mechanism underlying lymphomagenesis and it may represent a novel reliable and standardizable diagnostic tool in the characterization of similar diseases, also in the presence of scant material obtained from mini-invasive procedures.

#### ACKNOWLEDGEMENTS

We thank Sirja Moilanen for text editing. We also thank Cristiano Lanza and Vincenza Guzzardo for their excellent technical support. This work was supported by a grant from the University of Padua (Progetti di Ricerca di Ateneo 2010 and 2011), by the Veneto Region (Ricerca Finalizzata, 2006), and by the Cariparo Foundation Excellence-grant.

#### DISCLOSURE/CONFLICT OF INTEREST

The authors declare no conflict of interest.

1. A clinical evaluation of the international lymphoma study group classification of non-hodgkin's lymphoma. the non-hodgkin's lymphoma classification project. *Blood* 1997;89:3909–3918.
2. Horning SJ, Rosenberg SA. The natural history of initially untreated low-grade non-hodgkin's lymphomas. *N Engl J Med* 1984;311:1471–1475.
3. Acker B, Hoppe RT, Colby TV, *et al*. Histologic conversion in the non-hodgkin's lymphomas. *J Clin Oncol* 1983;1:11–16.
4. Lossos IS, Morgensztern D. Prognostic biomarkers in diffuse large B-cell lymphoma. *J Clin Oncol* 2006;24:995–1007.
5. Alizadeh AA, Eisen MB, Davis RE, *et al*. Distinct types of diffuse large B-cell lymphoma identified by gene expression profiling. *Nature* 2000;403:503–511.
6. Rosenwald A, Wright G, Chan WC, *et al*. The use of molecular profiling to predict survival after chemotherapy for diffuse large-B-cell lymphoma. *N Engl J Med* 2002;346:1937–1947.
7. Hans CP, Weisenburger DD, Greiner TC, *et al*. Confirmation of the molecular classification of diffuse large B-cell lymphoma by immunohistochemistry using a tissue microarray. *Blood* 2004;103:275–282.
8. Wahlin BE, Yri OE, Kimby E, *et al*. Clinical significance of the WHO grades of follicular lymphoma in a population-based cohort of 505 patients with long follow-up times. *Br J Haematol* 2012;156:225–233.
9. Chau I, Jones R, Cunningham D, *et al*. Outcome of follicular lymphoma grade 3: Is anthracycline necessary as front-line therapy?. *Br J Cancer* 2003;89:36–42.
10. Tada K, Kim SW, Asakura Y, *et al*. Comparison of outcomes after allogeneic hematopoietic stem cell transplantation in patients with follicular lymphoma, diffuse large B-cell lymphoma associated with follicular lymphoma, or de novo diffuse large B-cell lymphoma. *Am J Hematol* 2012) in press.
11. Ganti AK, Weisenburger DD, Smith LM, *et al*. Patients with grade 3 follicular lymphoma have prolonged relapse-free survival following anthracycline-based chemotherapy: the Nebraska lymphoma study group experience. *Ann Oncol* 2006;17:920–927.
12. Shustik J, Quinn M, Connors JM, *et al*. Follicular non-hodgkin lymphoma grades 3A and 3B have a similar outcome and appear incurable with anthracycline-based therapy. *Ann Oncol* 2011;22:1164–1169.
13. Piccaluga PP, Califano A, Klein U, *et al*. Gene expression analysis provides a potential rationale for revising the histological grading of follicular lymphomas. *Haematologica* 2008;93:1033–1038.
14. Sehn LH, Fenske TS, Laport GG. Follicular lymphoma: prognostic factors, conventional therapies, and hematopoietic cell transplantation. *Biol Blood Marrow Transplant* 2012;18(1 Suppl):S82–S91.
15. Fassan M, Croce CM, Rugge M. miRNAs in precancerous lesions of the gastrointestinal tract. *World J Gastroenterol* 2011;17:5231–5239.
16. Fassan M, Sachsenmeier K, Rugge M, *et al*. Role of miRNA in distinguishing primary brain tumors from secondary tumors metastatic to the brain. *Front BiosciSchol Ed*, 2011;3:970–979.
17. Lawrie CH, Chi J, Taylor S, *et al*. Expression of microRNAs in diffuse large B cell lymphoma is associated with immunophenotype, survival and transformation from follicular lymphoma. *J Cell Mol Med* 2009;13:1248–1260.
18. Culpin RE, Proctor SJ, Angus B, *et al*. A 9 series microRNA signature differentiates between germinal centre and activated B-cell-like diffuse large B-cell lymphoma cell lines. *Int J Oncol* 2010;37:367–376.
19. Roehle A, Hoefig KP, Reptsilber D, *et al*. MicroRNA signatures characterize diffuse large B-cell lymphomas and follicular lymphomas. *Br J Haematol* 2008;142:732–744.
20. Li C, Kim SW, Rai D, *et al*. Copy number abnormalities, MYC activity, and the genetic fingerprint of normal B cells mechanistically define the microRNA profile of diffuse large B-cell lymphoma. *Blood* 2009;113:6681–6690.
21. Okada H, Kohanbash G, Lotze MT. MicroRNAs in immune regulation—opportunities for cancer immunotherapy. *Int J Biochem Cell Biol* 2010;42:1256–1261.
22. Petrocca F, Vecchione A, Croce CM. Emerging role of miR-106b-25/miR-17-92 clusters in the control of transforming growth factor beta signaling. *Cancer Res* 2008;68:8191–8194.
23. Diosdado B, van de Wiel MA, Terhaar Sive Droste JS, *et al*. MiR-17-92 cluster is associated with 13q gain and c-myc expression during colorectal adenoma to adenocarcinoma progression. *Br J Cancer* 2009;101:707–714.
24. Hayashita Y, Osada H, Tatematsu Y, *et al*. A polycistronic microRNA cluster, miR-17-92, is overexpressed in human lung cancers and enhances cell proliferation. *Cancer Res* 2005;65:9628–9632.
25. Navarro A, Bea S, Fernandez V, *et al*. MicroRNA expression, chromosomal alterations, and immunoglobulin variable heavy chain hypermutations in mantle cell lymphomas. *Cancer Res* 2009;69:7071–7078.
26. Xiao C, Srinivasan L, Calado DP, *et al*. Lymphoproliferative disease and autoimmunity in mice with increased miR-17-92 expression in lymphocytes. *Nat Immunol* 2008;9:405–414.
27. Swerdlow SH, Campo E, Harris NL, *et al*. World Health Organisation Classification of Tumours of Haematopoietic and Lymphoid Tissues; International Agency for Research on Cancer press: Lyon, 2008.
28. Jaffe ES, Harris NL, Vardiman JW, *et al*. Hematopathology; Saunders Elsevier: Philadelphia, 2011.
29. Fassina A, Cappellesso R, Fassan M. Classification of non-small cell lung carcinoma in transthoracic needle specimens using microRNA expression profiling. *Chest* 2011;140:1305–1311.
30. Fassina A, Cappellesso R, Guzzardo V, *et al*. Epithelial-mesenchymal transition in malignant mesothelioma. *Mod Pathol* 2012;25:86–99.
31. Xiao C, Calado DP, Galler G, *et al*. MiR-150 controls B cell differentiation by targeting the transcription factor c-myb. *Cell* 2007;131:146–159.
32. Giannakakis A, Sandaltzopoulos R, Greshock J, *et al*. miR-210 links hypoxia with cell cycle regulation and is deleted in human epithelial ovarian cancer. *Cancer Biol Ther* 2008;7:255–264.



33. Fassan M, Volinia S, Palatini J, *et al*. MicroRNA expression profiling in human Barrett's carcinogenesis. *Int J Cancer* 2011;129:1661–1670.
34. Kagami Y, Jung J, Choi YS, *et al*. Establishment of a follicular lymphoma cell line (FLK-1) dependent on follicular dendritic cell-like cell line HK. *Leukemia* 2001;15:148–156.
35. Conconi A, Ponzio C, Lobetti-Bodoni C, *et al*. Incidence, risk factors and outcome of histological transformation in follicular lymphoma. *Br J Haematol* 2012;157:188–196.
36. Gascoyne RD, Adomat SA, Krajewski S, *et al*. Prognostic significance of bcl-2 protein expression and bcl-2 gene rearrangement in diffuse aggressive non-hodgkin's lymphoma. *Blood* 1997;90:244–251.
37. Kramer MH, Hermans J, Parker J, *et al*. Clinical significance of bcl2 and p53 protein expression in diffuse large B-cell lymphoma: a population-based study. *J Clin Oncol* 1996;14:2131–2138.
38. Skinnider BF, Horsman DE, Dupuis B, *et al*. Bcl-6 and bcl-2 protein expression in diffuse large B-cell lymphoma and follicular lymphoma: correlation with 3q27 and 18q21 chromosomal abnormalities. *Hum Pathol* 1999;30:803–808.
39. Rowley JD. Chromosome studies in the non-hodgkin's lymphomas: the role of the 14;18 translocation. *J Clin Oncol* 1988;6:919–925.
40. Korsmeyer SJ. Bcl-2 initiates a new category of oncogenes: regulators of cell death. *Blood* 1992;80:879–886.
41. Leich E, Salaverria I, Bea S, *et al*. Follicular lymphomas with and without translocation t(14;18) differ in gene expression profiles and genetic alterations. *Blood* 2009;114:826–834.
42. Hoeller S, Bihl MP, Zihler D, *et al*. Molecular and immunohistochemical characterization of B-cell lymphoma-2-negative follicular lymphomas. *Hum Pathol* 2012;43:405–412.
43. Yunis JJ, Mayer MG, Arnesen MA, *et al*. Bcl-2 and other genomic alterations in the prognosis of large-cell lymphoma. *N Engl J Med* 1989;320:1047–1054.
44. Huang JZ, Sanger WG, Greiner TC, *et al*. The t(14;18) defines a unique subset of diffuse large B-cell lymphoma with a germinal center B-cell gene expression profile. *Blood* 2002;99:2285–2290.
45. Freedman A. Follicular lymphoma: 2011 update on diagnosis and management. *Am J Hematol* 2011;86:768–775.
46. Baffa R, Fassan M, Volinia S, *et al*. MicroRNA expression profiling of human metastatic cancers identifies cancer gene targets. *J Pathol* 2009;219:214–221.
47. Demirkesen C, Tuzuner N, Esen T, *et al*. The expression of IgM is helpful in the differentiation of primary cutaneous diffuse large B cell lymphoma and follicle center lymphoma. *Leuk Res* 2011;35:1269–1272.
48. He L, Thomson JM, Hemann MT, *et al*. A microRNA polycistron as a potential human oncogene. *Nature* 2005;435:828–833.
49. Ota A, Tagawa H, Karnan S, *et al*. Identification and characterization of a novel gene, C13orf25, as a target for 13q31-q32 amplification in malignant lymphoma. *Cancer Res* 2004;64:3087–3095.
50. Neat MJ, Foot N, Jenner M, *et al*. Localisation of a novel region of recurrent amplification in follicular lymphoma to an approximately 6.8 mb region of 13q32-33. *Genes Chromosomes Cancer* 2001;32:236–243.
51. Ji M, Rao E, Ramachandradeddy H, *et al*. The miR-17-92 microRNA cluster is regulated by multiple mechanisms in B-cell malignancies. *Am J Pathol* 2011;179:1645–1656.